



Construction of Human Head Models for Anthropometry and Dosimetry Studies of Hand-Held Phones

J Márquez^{1,3}
T Bousquet²
I Bloch¹
F Schmitt¹
and Grangeat C²

¹ TSI Dept., Ecole Nationale Supérieure des Télécommunications, 46 rue Barrault, 75634 Paris Cedex 13, France.

² Dosimetry Dept., Alcatel Corporate Research Center, Route de Nozay, 91461 Marcoussis, France.

³ Centro de Instrumentos, UNAM. marquez@enst.fr

Artículo recibido 28/noviembre/2000
Artículo aceptado 5/enero/2001

ABSTRACT

Laser-scan acquisitions were obtained from real human heads and processed for the construction of a database of anthropomorphical phantoms for dosimetry studies of hand-held mobile phones. Raw data was converted to cylindrical range images and several image processing techniques were then applied to filter and smooth the profiles for 3D-model construction. A triangulated surface was then obtained for rendering each phantom, and for CAD and finite-element simulations; we also built a discrete volume representation for FDTD analysis (Finite Differences in Time Domain). The ear region was isolated and labeled for special treatment. At the end of this paper, two applications of head phantoms are also briefly presented, concerning dosimetry and anthropometry problems.

Key words:

Dosimetry, Anthropometry, Human-head models, Phantoms, Hand-held phones.

RESUMEN

Se obtuvieron adquisiciones de escáner láser de cabezas humanas reales las cuales se procesaron para construir una base de datos de fantasmas antropomórficos para estudios de dosimetría de teléfonos celulares. Los datos brutos fueron convertidos a imágenes de profundidad cilíndricas y se aplicaron varias técnicas de procesamiento de imágenes para filtrar y suavizar los perfiles para la construcción de modelos 3D. Se obtuvo una superficie triangulada que permitió el rendering de cada fantasma, así como simulaciones en CAD y elementos finitos; se construyó también una representación en volumen discreto para análisis DFDT (Diferencias Finitas en el Dominio del Tiempo). La región del oído fue aislada y etiquetada para un tratamiento especial. Al final de este artículo se presentan brevemente dos aplicaciones de los fantasmas de cabezas que tienen que ver con problemas de dosimetría y antropometría.

Palabras claves:

Dosimetría, Antropometría, Modelos de cabezas humanas, Fantasmas, Teléfonos celulares.



INTRODUCTION

Besides phone terminal positioning and other variables, radio-frequency wave absorption by the human body head depends on anatomical complex features, in particular at the ear and mouth regions. Homogeneous phantoms representing the user have been previously used,¹ and accuracy improvements up to 2 mm precision resolution from MRI (Magnetic Resonance Imaging) scans have been made.² However, these studies are based on a single morphological average from army anthropometrical data from male subjects, not representative of the population of mobile phone users. Individual head models from 3D laser scan acquisitions of human subjects will allow simulation of power absorption in anthropomorphic phantoms of several subjects. In particular, we are interested in estimating the maximum SAR value (Specific Absorption Rate) and its distribution inside the head, in the proximity of the ear. Besides construction method results, we present at the end some preliminary results of dosimetric (SAR spatial distribution) and anthropometric applications.

Objectives: Our first goal was the development and application of methods for building a data base of 3D human head profiles from laser-scan acquisitions and with refined analysis in the region of the ear. The final goals of this study are to collect anthropometrical data of the head with collapsed ear for standardization of the head model and to investigate by simulation the dispersion of interactions of hand-held mobile phones with the human head.

The present work was part of the European federative project COMOBIO, as a collaboration between the Ecole Nationale Supérieure des Télécommunications (ENST, Paris) and the Alcatel Corporate Research Center, (Marcoussis laboratories). We present in the following paragraphs some of the methods we developed for head model construction, morphometry and feature extraction. Further details are found in references 5 and 6.

METHODS

Laser-scan acquisition protocol

The numerical acquisition of human heads was performed with a 3D laser scanner from Cy-

3D Head Data Base with Collapsed Ear



- 3D scanning of 41 people
- Precision of measurements: 1 mm
- Triangular meshing & FDTD voxels (1mm)

Figure 1. Laser-scan acquisition setup, with collapsed ear, and surface-mesh rendering for each head phantom after model construction and refinement.

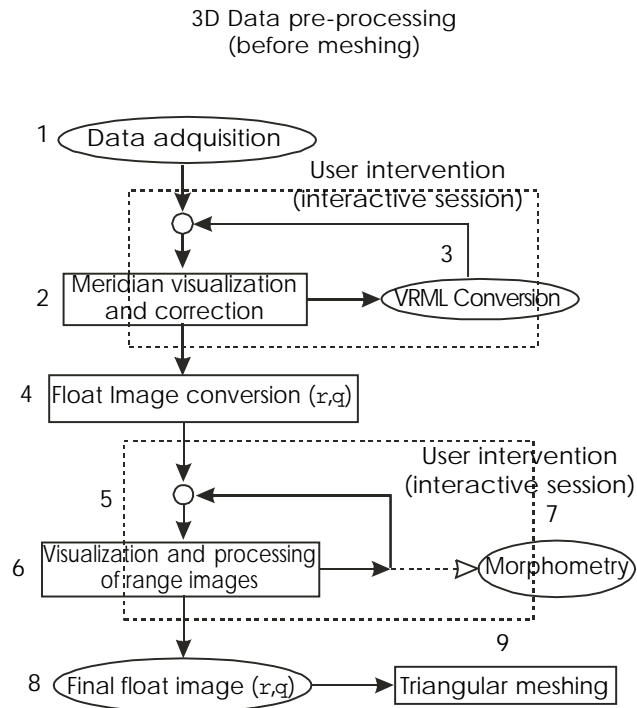


Figure 2. 3D Data pre-processing stages. See text for detailed steps (side numbers). Dashed rectangle is zoomed in figure 3.

berware,³ with the assistance of Dr. M. Nahas, from the Paris VII University. Anthropometric information of subjects was recorded (weight, age, sex, height), and no specific selection was done at all, having a representative assortment of world-population. Figure 1 shows the acquisition setup, with physical landmarks to reproduce the same position for all subjects. The scanner rotates around the head axis, producing distance information of the 3D relief. Two 3D renderings of sample phantoms are also shown at right. During acquisition sessions, the ear configuration was either in its natural position or the superior lobe was pressed against the skull for representing the external shapes in use of collapsed by a mobile phone. The hair of each subject was covered by an elastic bathing cap and use of earrings was allowed. The best of two acquisitions was retained, and 45 subjects were scanned, but we retained 41, with 12 women in the final sample. Raw acquisition data consists of meridian profiles, with varying number of points, depending on relief. Spacing Δy between points is less than 1 mm in height by projection, and less than 0.5 mm in an-

gular position α . Depth differences Δr may vary widely (several millimeters), especially at the skullcap, under the chin and behind the ears.

Cylindrical range-image processing

Before model construction (meshing or voxelization), several pre-processing operations are performed. Floating range images of 480x580x5-byte resolution were extracted from the raw scan data, in order to filter out artifacts and noise, preserving accuracy, and locate morphological features in image space and then in object space. The range-image representation is also convenient for other manipulations and measurements, since 3D information is displayed in the Mercator cylindrical projection as a gray-level image, as shown in figure 4 (top), where the relations between coordinates systems are explained. Global steps towards phantom construction (triangular meshing) are shown in figure 2. These include format conversions and image processing techniques, applied to range images, where gray level codes depth (or height, from the rotation axis of the head).

Figure 4 (Bottom): Shows the helicoidal image correction, in the general case. (a) In object space the cylindrical mismatching presents two components, Δy , Δr , or in other words, two values rD_1 , rD_2 at $y = 0$ and $y = y_{\max}$. (b) The most significant mismatch in range images is rD , made visible in gray levels about the closing meridian ($\alpha = 270^\circ$, $x' = 358$). An error $\Delta \alpha$ is also possible. (c) A circular, closing correction in r is made for each contour $y' = \text{constant}$. An example of this correction is shown later.

Processing of range images (step 5, 6 and 7 in Figure 2, zoomed in Figure 2) includes: defect correction, smoothing and filtering of artifacts, restoration of missing information (holes), statistics and morphometry (steps 5 and 6 of Figure 3). Filtering and smoothing with float-precision include Gaussian convolution in cylindrical coordinates, and linear interpolation in image space. Measurements include statistics about ear features (regional depth, for example). Details are given in reference 5.

Some corrections are automatic, but since each subject has different morphology and each acquisition poses specific problems, user intervention was required to choose ROI (Region Of Interest) windows for restoration and filtering (steps 2, 3 and 4 in Figure 3).

Since there may be alignment mismatch between starting and ending acquisition meridians,

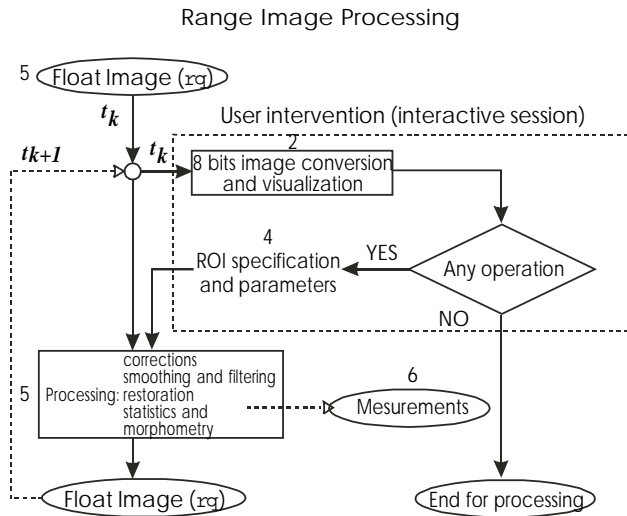


Figure 3. Range-image processing steps.

a special procedure called helicoidal mismatch correction was developed (Figure 4, bottom). There may be also outlayer points, which are discarded by median filtering of meridian contours (step 2 of Figure 2). 3D visualization of acquisition data is done by conversion to VRML format. Figure 5 shows an example of typical defects to be corrected, filtered or missing parts to be restored by local bilinear interpolation (lofting in x or in y directions, from bounding depth profiles). Earrings are also “erased”, but may be taken into account since power absorption characteristics may change.

Specific extraction and manipulation of the ear region

A boundary rectangular zone around the ear was used as a reference surface for the ear structure. Using first-order surface fitting, the simplest approximated patch to replace the ear structure is was a Bilinearly Blended Coons patch,⁴ which is built from the four boundaries and corners of the reference surface, as illustrated by figure 8.

The construction method of Coon combines orthogonal lifting of bounding contours and a standard bilinear interpolator of the 4 corners, obtaining, by cross modulation, the spline surface resulting from a tensor product of the bounding contours. The resulting surface interpolates the cranium at the ear region and a gradual smoothing of the ear can be achieved by blending from 0.0 (no ear) to 1.0 (detailed ear), without modifying other regions of the head phantom. This referen-

Range-Image Representation of Laser-Scan Acquisitions

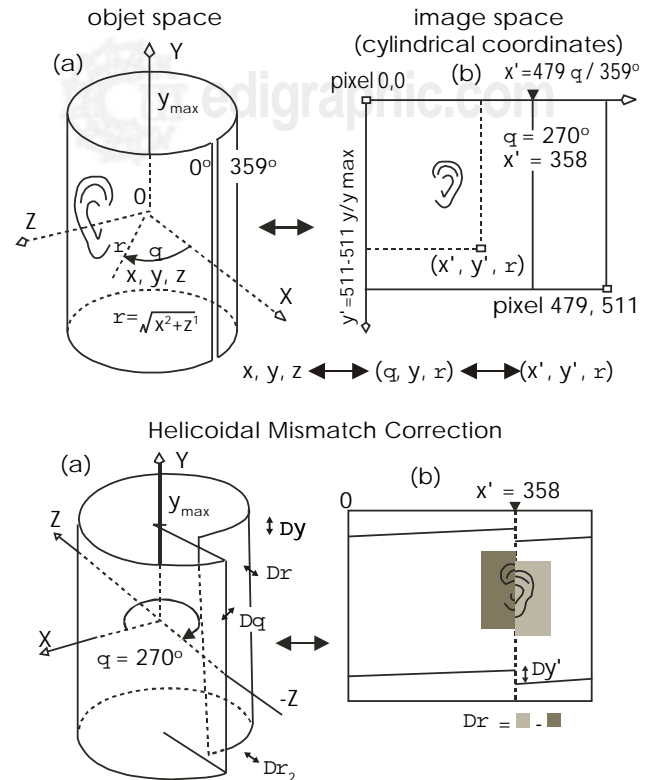


Figure 4. (Top) is a diagram of coordinate systems in a cylindrical Mercator projection (a) Points (x, y, z) in object-space and in cylindrical coordinates (α, y', r) ; (b) coordinates in image-space (x', y', r) , where elevation (rather than range-depth) r is represented for display by gray levels normalized in $[0,255]$. Columns $x' = \text{constant}$, correspond to meridians $(\alpha \text{ fixed})$, and lines (or image rows) $y' = \text{constant}$, are the “parallels”. The 2D-image is a matrix of 480 x 512 pixels. Inverted orientation for image axes correspond to display software xv (“Xview”), in order to correctly display a head. Meridian $\alpha = 27^\circ$ is the starting/ending meridian for acquisition.

ce surface serves also to define a “zero-ground-zero” for thickness estimations of the ear at various locations. The ear structure in figure 6 is thus “extracted”, as shown in figures 9.

Triangular meshing

The 3D model of each head was built with regular meshes by Eulerian triangulation of the range image, at two mesh resolutions: a coarse one, averaging 8 mm at triangle diagonals, and a fine one located at the ear region, averaging 4 mm. A random diagonal swapping, visible in figure 6, is required to suppress or reduce parasitic

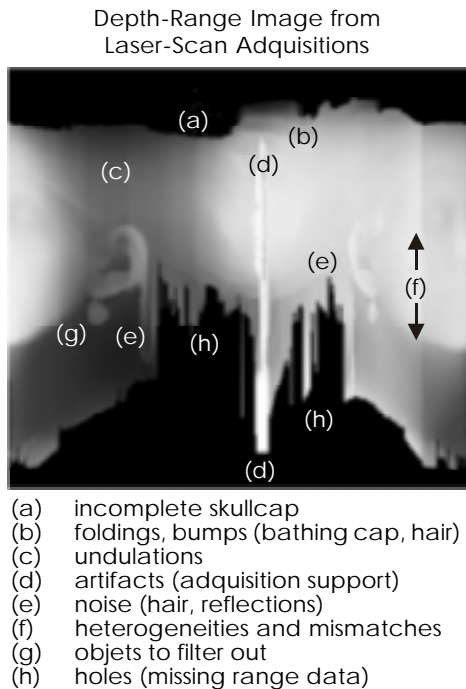


Figure 5. Several defects and artifacts to be corrected or filtered in the depth-range image from laser-scan acquisitions. Missing areas are interpolated from available surface information.

couplings occurring in finite-element simulations. Diagonal size is limited by Eulerian subdivision, but no other mesh simplification is done. Transitions between different mesh resolutions are solved by look-up tables of node and triangle configurations, to keep the Eulerian property. Figure 7 pre-

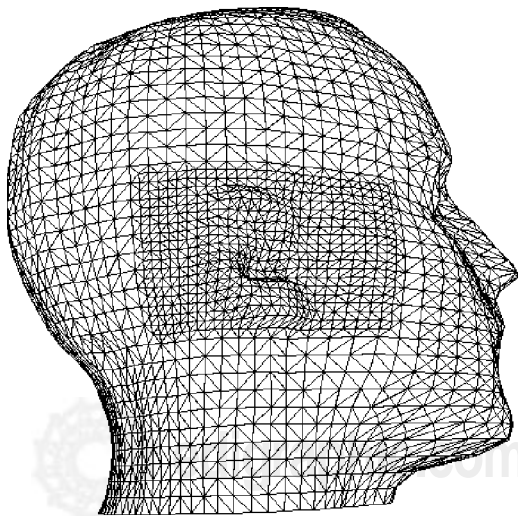


Figure 6. 3D-rendering of the triangular mesh model with a fine resolution in the ear region.



Figure 7. VRML-format sample of triangulated mesh, partially corrected (requires a VRML browser, Vers.1.5 or higher).

sents a final color rendering of a phantom with medium smoothing. Interactive rendering is done with a commercial browser for VRML (Virtual Reality Modeling Language) format. Superposition of phantom models with ear extraction by Coons interpolation of cranium is rendered in figure 10.

Conversion to discrete representation or "voxelization"

Triangular meshes simplify model complexity, it allows integration of data to CAD systems and speed up interactive visualization of phantoms. However, a discrete volume representation is still needed for several reasons. Voxelization of a mesh allows to simulate the dispersion of electromagnetic radiation in the interior of a discrete grid with two medium components (air and head tissue) and an interface (the surface of the head). Voxels are also useful to label distinct head components and spatial configurations, as described in figure 13, in order to evaluate dosimetry with and without the ear, and the effect of ear collapse, as pressed by a hand-held phone during normal operation. Furthermore, topological problems (v.g. voxel connectivity) at high resolution is tackled with discrete Mathematical Morphology operators.

Within the framework of a voxel representation, the use of discrete 3D distance fields open the possibility of accurate error evaluation in dosimetric applications, and similarity comparisons in

Interpolation Filters and Bilinearly-Blended Coons Patches by Orthogonal Lifting

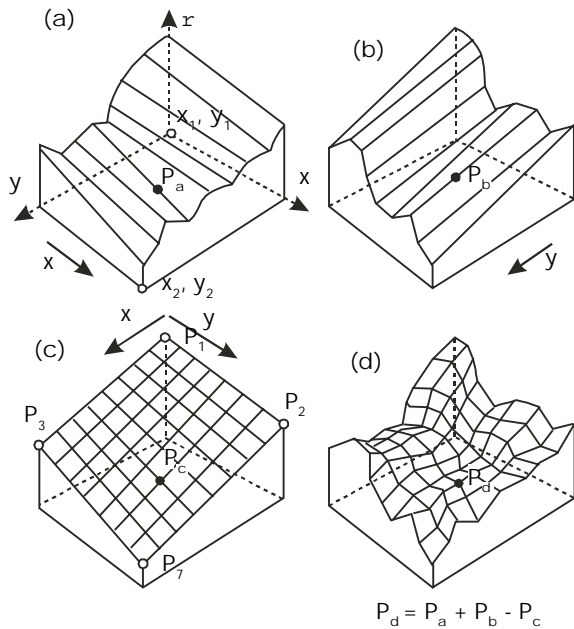


Figure 8. Diagram describing the construction of the bilinearly blended Coons patch, using spline-tensor products (horizontal plus vertical lofts minus bilinear interpolated plane).

volume subsets for anthropometric problems. In fact, the distance-field approach was employed for ear-shape averaging, as described in the Application II section.

Figure 12 summarizes the process for voxelization of surface meshes. Volume labelling, connected-component extraction, mosaic visualiza-

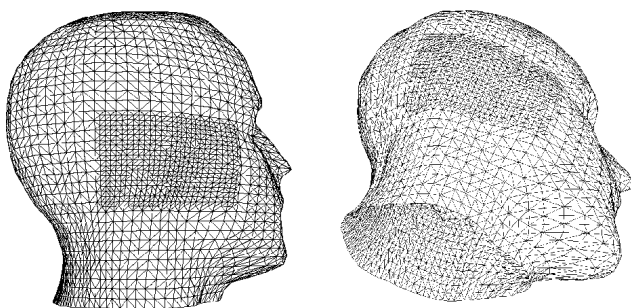


Figure 9. Two views of a head model with the ear structure replaced by a bilinearly-blended Coons patch interpolator in the high-resolution region. Note that the interpolated cranium effectively interpolates the surface between the bounding contours, made visible by higher resolution. The Coons patch is inside the high-resolution region.



Figure 10. Superposition of mesh models with ear (orange) and without ear (light gray) on the interpolated region.

tion and other operations were performed using the TIVOLI software package of the TSI department of the ENST and other software by the authors. Figure 13 shows a 3D rendering of a voxelized phantom, with color labels of separated ear, interior, exterior and symmetric difference between a head with and without ear.

Figure 14 shows the visual superposition of a triangular mesh and discrete volume information (component labels are represented by colored dots per voxel site). Spatial relationships are better appreciated in an interactive animated rendering, using a VRML browser.

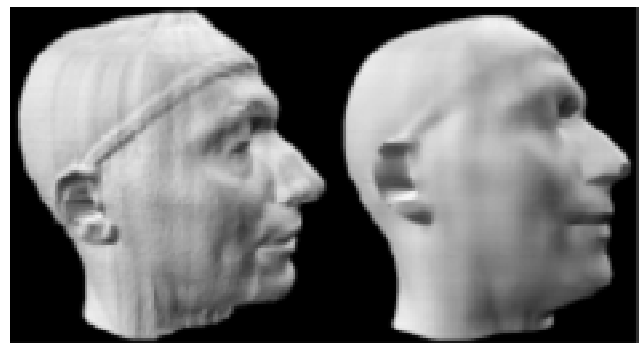


Figure 11. 3D Rendering (mesh of 8mm and 4mm resolution) before and after gaussian smoothing in range-image space.

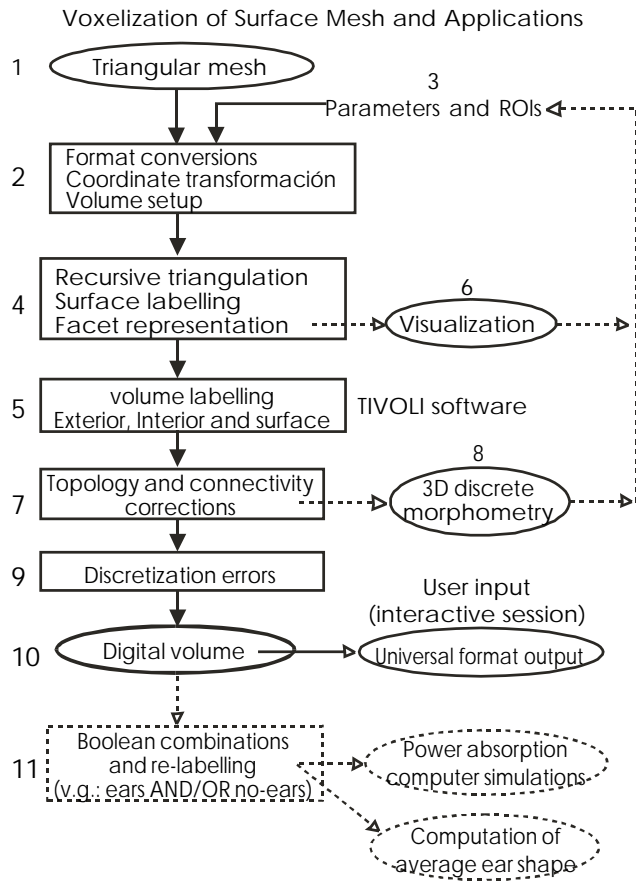


Figure 12. Discrete representation: voxelization stage of the mesh.

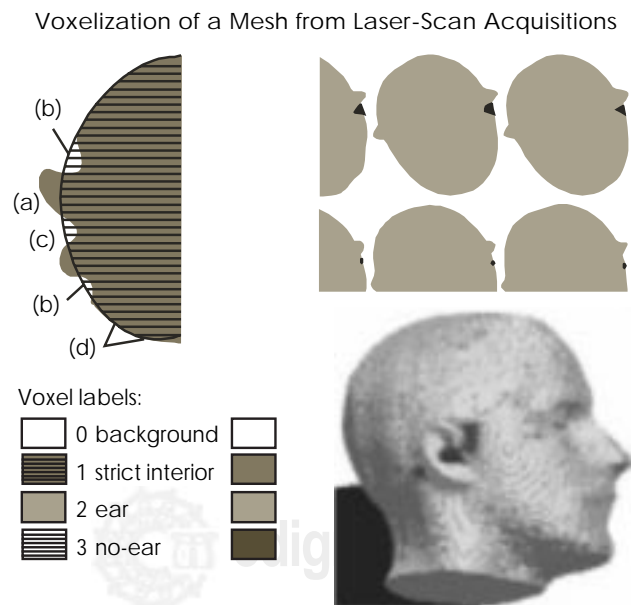


Figure 13. Assignment of voxel labels on discrete representations of a head with/without ear.

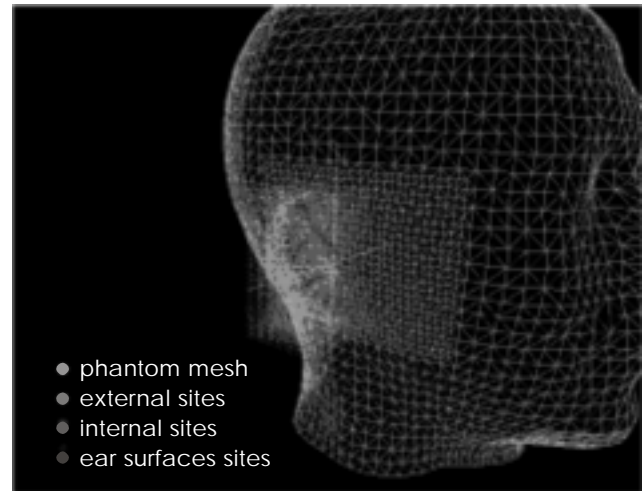


Figure 14. Sites of voxelized components with exterior/interior/surface labels superposed on the original mesh. Color of voxel sites represent different volume components.

RESULTS

A database of 40 human head profiles was obtained in two basic formats: a triangulated surface and a discrete volume representation at 2-mm precision resolution for FDTD simulations. A third raw-data representation (meridian profiles) is also available for other kinds of anthropometrical studies. Meshes are represented in VRML (Virtual Reality Modeling Language) format and Universal (Ideas software) format. A color image ("texture map") of each subject is also available for VRML 2.0 browsers. Several 2D and 3D processing tools were developed to solve acquisition problems and investigate morphologic properties of the sampled population, particularly in the region of the collapsed ear for the application to standardization issues of SAR measurements of mobile phones. In the following paragraphs we describe present applications of the phantom database. Morphometric methods and results of ear thickness estimations are at present confidential information, but should be disclosed in a future publication. A detailed technical report⁶ and the full database in CD-ROM are available for research applications from the TSI Department, ENST.

Applications of the human head database

Facial details are smoothed in the phantoms as required in present work, preserving volume, re-

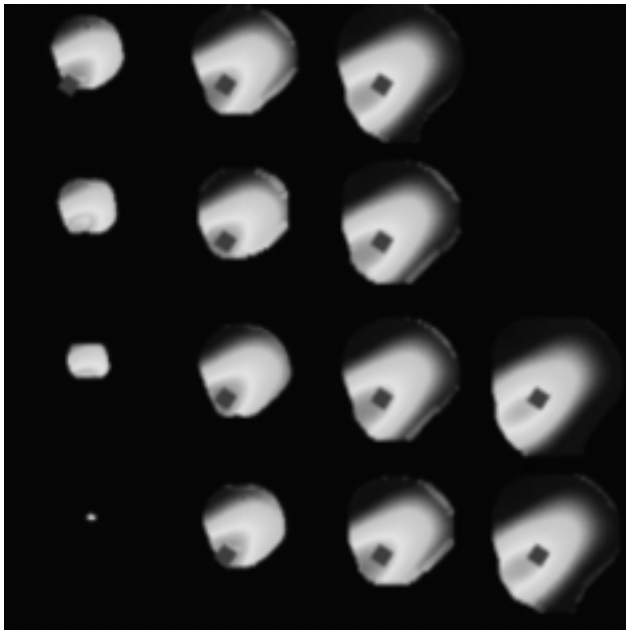


Figure 15. Application 1: Simulation and experimental validation of SAR (Specific Absorption Rate) value distribution on a Phantom. 16 samples of discrete volume distribution of SAR are shown. The red squares are slices of the cubic probe, where local SAR average is maximum within the volume (actual Z-resolution is higher).

ducing information overhead, but minimizing errors with respect to original acquisition data (meridian clouds of points). Higher resolution meshes may be obtained with the same procedures, and other zones than the ear may be analyzed. Two applications of the digital database of human heads are developed at present, in France and Mexico.

Hand-held phone dosimetry

Radio-frequency field absorption of GSM and other emission devices is simulated inside the head, using homogenous tissue models and full-detailed head atlases from MRI acquisitions. Such simulations are currently done by partners of the COMOBIO project, using also our head phantoms.^{8,9} We ourselves developed software to calculate the regions of maximum SAR value, averaging inside a cubic “probe” representing 1 and 10 g of intracranial mass. This probe scans the head interior, with a face lying on the internal surface, following standard protocols of dosimetry. Its orientation is quantized to seek the maximum local average of SAR values. Experimental measurements on physi-

cal realizations of generic phantoms allow to validate simulation results, extracting error differences between simulation volume and tri-linearly interpolated volumes from experimental samples. Figure 15 shows some sampled slices of the spatial distribution of power absorption simulations inside a voxelized phantom.

Specific anthropometry of populations: Ear-shape averaging

A second application of the database consists in the construction of a robust morphological average of the human ear over a subset of the database. Such an averaged shape is obtained progressively, with a weighted contribution which penalizes those ears whose shape deviates too much from the accumulated average. In order to average corresponding features, geometric registration of the ears and scale normalization are applied using PCA (Principal Component Analysis). Morphological averaging is based in an innovative method called Progressive Morphological Blending, which in turn generalizes the method of morphological interpolation used in atlas construction by means of level sets. Our method averages Euclidean-distance fields in 4D: three dimensions account for the ear shape and the fourth dimension is the interpolation range between ears. We recently validated our average ear characteristics, comparing with the Standard of Anthropomorphical Model (SAM), proposed in June 2000 by the BioElectroMagnetic Society (BEMS). The SAM phantom do not has a realistic human ear, but a simplified “mesa” of specific thickness. Our averaged ear is the first

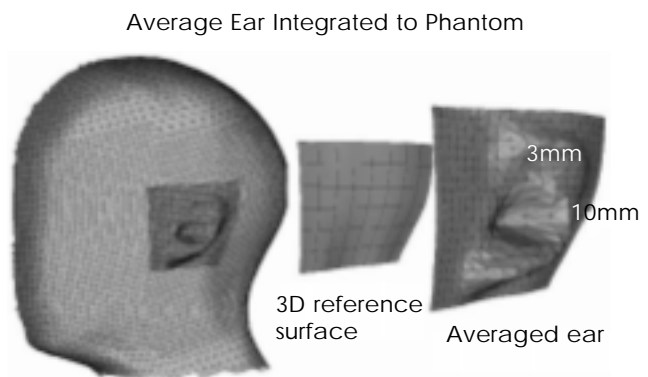


Figure 16. Application 1: Construction of an average anatomical feature (the ear of 24 individuals), to be integrated to a generic phantom.

obtained from real human heads by morphological averaging. The theory and algorithms of this application are described elsewhere.⁷

Acknowledgements

This research was sponsored by the French government within the COMOBIO project (RNRT program: National Network for Research on Telecommunications). We thank Dr. Monique Nahas from the Laboratoire Universitaire des Applications de la Physique, Université Paris VII, for laser-acquisition assistance.

REFERENCES

1. Grangeat C et al. Radio-frequency radiation from mobile phones, *Alcatel Telecommunications Review*, 4th Quarter 1998: 298-304.
2. Wiart J et al. Calculation of the power deposited in tissues close to a handset antenna using non uniform FDTD, *Proceedings of the Second World Congress for Electricity and Magnetism in Biology and Medicine*, Bologna, June 97, Plenum Press.
3. Inc. Cyberware Laboratory, 4020/rgb 3d. scanner with color digitizer, available information at <http://www.cyberware.com/pressReleases/index.html>, 1990.
4. Barnhill R. Coons patches and convex combinations, in Les Piegl, editor. *Fundamental Developments of Computer Aided Geometric Modeling*. Academic Press, London, 1993.
5. Márquez J, Bousquet T, Bloch I, Schmitt F and Grangeat C. Laser-Scan Acquisition of Head Models for Dosimetry of Hand-Held Mobile Phones. Poster No. 25, *BioElectromagnetics Society, 22th Annual Meeting*, Technical University, Munich, Germany. Abstract Book (Technical University, Munich). 2000: 123.
6. Márquez J, Bloch I, Schmitt F. IPCYL: Logiciels de traitement de données cylindriques et images en profondeur, MakeTri et Voxelize: maillage triangulaire et voxelization pour la création de fantômes antropométriques. Description des méthodes et documentation des logiciels (Vers. 1.0). Dept. IMAGES, ENST, Paris, octobre 1999.
7. Márquez J, Bloch I, Bousquet T, Grangeat C, Schmitt F. Morphological Robust Average of the Ear Shape of Human-Head Phantoms. In preparation. January, 2001.
8. Dale C, Monebhurrin V, Chaillou S, Bolomey J, Wiart J. Representativity of Homogeneous Phantoms in Testing Compliance of Mobile Phones to SAR Limits. *BioElectromagnetics Society, 22th Annual Meeting*, Technical University, Munich, Germany. Abstract Book (Technical University, Munich): 2000: 19.
9. Hilali N. Traitements de mesures 3D de champ électromagnétique dans un fantôme de la tête et calcul du SAR. Rapport de stage, DEA, Université Paris XII-Val de Marne et le Dept. TSI,ENST Paris. Sous la responsabilité de Isabelle Bloch, Thierry Bousquet et Jorge Márquez. Septembre 1999.